

X-ray emission from clusters of galaxies and cosmological parameters

K P SINGH

Tata Institute of Fundamental Research, Homi Bhabha Road, Mumbai 400 005, India

Abstract. Clusters of galaxies are excellent probes of cosmic structure and evolution. X-ray studies of clusters provide some of their key parameters, viz., temperature of the hot intra-cluster gas, its metallicity, X-ray luminosity and surface brightness giving mass distribution and mass-flow rate in the case of cooling flows. X-ray measurements for a large sample of clusters have led to estimates of the total gravitating mass in them, which can be compared to the virial masses derived from dynamical considerations and gravitational lensing in some of them. X-ray derived total masses are consistent with masses obtained from the other methods after the effects due to the presence of cooling flows are taken into account in the analyses. Estimated virial masses, lack of evolution in X-ray properties, and detection of several very hot clusters at high redshifts indicate a Universe with a low value (≤ 0.3) for the Ω parameter.

Keywords. Clusters of galaxies; X-rays.

PACS No. 2.0

1. Introduction

Clusters of galaxies are the most massive bound systems in the Universe. With their typical sizes of 1–3 Mpc, they are ‘fair’ samples of the Universe, and represent the ‘gross’ properties like mass and baryon fraction of the Universe. Formed at an early epoch, clusters of galaxies retain the ‘imprint’ of their formation histories since their dynamical timescales are comparable to the age of the Universe. Unlike galaxies, which are certainly open systems, clusters of galaxies do not lose material as they evolve from pre-collapse systems, and thus qualify for being called as ‘closed’ systems. By virtue of these properties they provide basic data for the study of formation of elements in the Universe. Therefore, studies of evolution, temperature, luminosity function, mass and chemical enrichment of clusters of galaxies can place strong constraints on theories of large scale structure formation and evolution, and on cosmological parameters such as Ω and Λ .

Historically, clusters of galaxies were detected and classified on the basis of their optical appearance leading to well known catalogues by Abell [1] and Zwicky [2]. These methods suffered a great deal from the risk of projection effects leading to missing out of poor clusters and improper estimation of richness of clusters in several cases. Hot intra-cluster gas visible in X-rays and trapped inside the cluster gravitational potential provides a sure indication that the system is indeed bound in three dimensions. Primarily caused by

bremsstrahlung, X-ray emissivity (Σ_X) is proportional to the square of the ion density and thus much more peaked at the gravitational centre of the cluster than the projected galaxy distribution. Therefore, clusters need to be almost perfectly aligned along the line of sight if they are to be mistaken for a single more luminous object. X-ray surveys thus provide a more efficient and less unbiased way of compiling cluster samples when compared to optical surveys due to: (a) absence of projection effects; (b) trapping and heating of gas in a bound system; (c) concentration of the X-ray flux towards the gravitational centre of the cluster.

X-ray emitting gas constitutes a major component of the baryonic matter in clusters of galaxies. The mass of the X-ray gas is 1–5 times the mass seen in the visible, and contributes about 5–25% of the total cluster mass [3] which is in the range of 10^{14} – $10^{15}M_\odot$. X-ray observations of clusters can be used to study the evolution of their properties like luminosity function, mass, temperature and chemical enrichment.

2. X-ray observations

2.1 A brief history

Since the early discoveries of X-ray emission from M87 in the Virgo cluster in a rocket flight in 1965, Coma cluster in 1969, and NGC 1275 in the Perseus cluster in 1970, study of X-ray emission from clusters of galaxies has made significant and substantial progress with the use of satellite-borne imaging and spectroscopic X-ray detectors. These satellite-borne instruments include X-ray telescopes and detectors on the Einstein observatory, OSO-8, EXOSAT, Tenma, Ginga, ROSAT and ASCA. Presently, there are excellent soft X-ray images of about 100s of clusters taken with ROSAT, and good quality medium-resolution energy spectra of ≥ 50 clusters taken with ASCA. ROSAT has provided us with the first all-sky X-ray survey of galaxy clusters [4,5]. Limited X-ray surveys for galaxy clusters in selected regions of the sky were carried out previously with the Einstein observatory and most recently with ROSAT [6,7]. Several new clusters of galaxies have also been detected serendipitously in the ROSAT fields and identified optically [8,9].

2.2 Cluster parameters from X-ray imaging and spectroscopy

Observations with X-ray imaging telescopes and detectors with low-to-medium spectral resolution find hot (10^7K – 10^8K) thermal gas extended over the intracluster space covering sizes of 1–3 Mpc. X-ray images provide us with the surface brightness distribution of the hot gas. As an example, X-ray surface brightness map of the highest redshift ($z = 0.83$) cluster in the Einstein Medium Sensitivity Survey (EMSS), known as MS1054-0321, taken with ROSAT High Resolution Imager (HRI) is shown as contours superposed on an I-band image in figure 1 taken from [10]. X-ray contour levels shown correspond to surface brightnesses of 14, 3.9, 11.6, and $14.0 \times 10^{-14} \text{ erg cm}^{-2} \text{ s}^{-1} \text{ arcmin}^{-1}$.

Assuming azimuthal symmetry of X-ray emission, radial surface brightness profiles can be generated and modeled using hydrostatic-isothermal models [11]. In these models, both X-ray emitting gas and galaxies are assumed to be in hydrostatic equilibrium and each is isothermal. It is further assumed that the galaxies are in equilibrium with the total

gravitational mass. Using King's approximation [12] to the isothermal sphere, the X-ray surface brightness distribution is then given by

$$S(r) = S(0)[1 + (r/a)^2]^{-3\beta+0.5} \quad (1)$$

where 'a' is the cluster core radius, β is the ratio of the energy per unit mass in galaxies to the energy per unit mass in gas and is given by

$$\beta = \mu m_H \sigma^2 / 3kT_X \quad (2)$$

where μ is the mean molecular weight, m_H is the mass of the hydrogen atom, σ is the three-dimensional (space) cluster velocity dispersion, k is the Boltzmann's constant, and T_X is the mean X-ray gas temperature. Fitting the above model to the radial surface brightness profiles gives us the core radius and β value for a cluster, which then can be used to estimate the gas mass as well as the total mass of the cluster. The gravitating mass of the cluster is given by

$$M(< r) = 1.13 \times 10^{15} \beta h^{-1} [T_X/10 \text{ keV}] [r/10 \text{ Mpc}] (r/a)^2 / (1 + (r/a)^2) M_\odot \quad (3)$$

where $h = H_0/100$, and H_0 is Hubble constant in units of $\text{km s}^{-1} \text{Mpc}^{-1}$ (see [7]). Thus, X-ray images help determine structure, mass and morphology of clusters.

X-ray spectroscopy tells about the temperature and chemical enrichment of the gas. For example, MS1054-0321 shown in figure 1 is very hot with $T_X = 12.3_{-2.2}^{+3.1}$ keV ($1 \text{ keV} = 1.16 \times 10^7 \text{ K}$) as measured with ASCA [10]. Combined with velocity dispersions measured optically, the temperature measurements give us an estimate of the β value independent of that obtained from model fit to X-ray radial profiles (see eqs. above). Measurements of the redshifts of 12 galaxies marked in figure 1 using Keck and Canada–France–Hawaii telescopes lead to a value of $1360 \pm 450 \text{ km s}^{-1}$ for the velocity dispersion of MS1054-0321 cluster [10].

In general, there is a fairly good correlation between the X-ray temperature and velocity dispersion as shown in figure 2 [13]. This indicates that, to first order, gas and galaxies are in the same gravitational potential and that anisotropies and radial gradients in the velocity tensor of galaxies are not very large. However, a significant scatter in the distribution can be seen in the figure 2. Bahcall and Lubin [14] pointed out that the use of King approximation for the galaxy distribution had lead to a discrepancy between the values of β obtained from two methods, and is resolved if the galaxy distribution, $\rho_{\text{gal}}(r) \propto r^{-2.4 \pm 0.2}$.

Spatially resolved X-ray spectroscopy is required for the determination of temperature profiles and is ideal as it leads to a measure of the mass of X-ray gas as well as the total cluster mass without the assumption of isothermality. For a spherical system in hydrostatic equilibrium the enclosed cluster mass is

$$M(< r) = kT(r)r/G\mu m_H [(d \log \rho / d \log r) + (d \log T / d \log r)] \quad (4)$$

where ρ and T are the density and temperature profiles. Radial temperature profiles are available for 30 nearby clusters [15], but there are significant uncertainties in the outer regions ($r \geq 1 \text{ Mpc}$). More such profiles would become available after the launch of AXAF and XMM. Detection of X-ray line emission through medium-to-high resolution spectroscopy leads to estimates of elemental abundances and thus chemical enrichment of

cluster gas. ASCA spectra show that the mean abundance of Fe is 0.28 solar (photospheric value) and Si/Fe ratio is 2.2 ± 0.25 solar, which is consistent with most metals being created in type II supernovae [16].

2.3 Cooling flow and its effects on cluster parameters

X-ray emission from a cluster, thus cooling of gas, due to thermal bremsstrahlung and line emission depends on the square of the gas density which increases towards the central regions. The cooling time-scale which is $\propto T/(\rho \Sigma_X)$, becomes smaller than the age of the cluster in the core ($a = 30\text{--}300$ kpc) of the cluster. As the gas cools more efficiently in the core, it results in an inward flow due to gravity and thermal pressure and to stay in pressure equilibrium with the outer layers. Such cooling flows are found in the cores of 60–90% clusters [17,15]. X-ray imaging spectroscopy has confirmed the presence of cooling flows by finding decreasing temperatures inside the cluster cores [15]. Cooling flow in the core thus appears to be the natural state for a regular, relaxed cluster which perhaps can only be disrupted by a major merger event. Multi-phase cooling gas in the cluster core has important consequences for the analysis of X-ray data, in particular for the determination

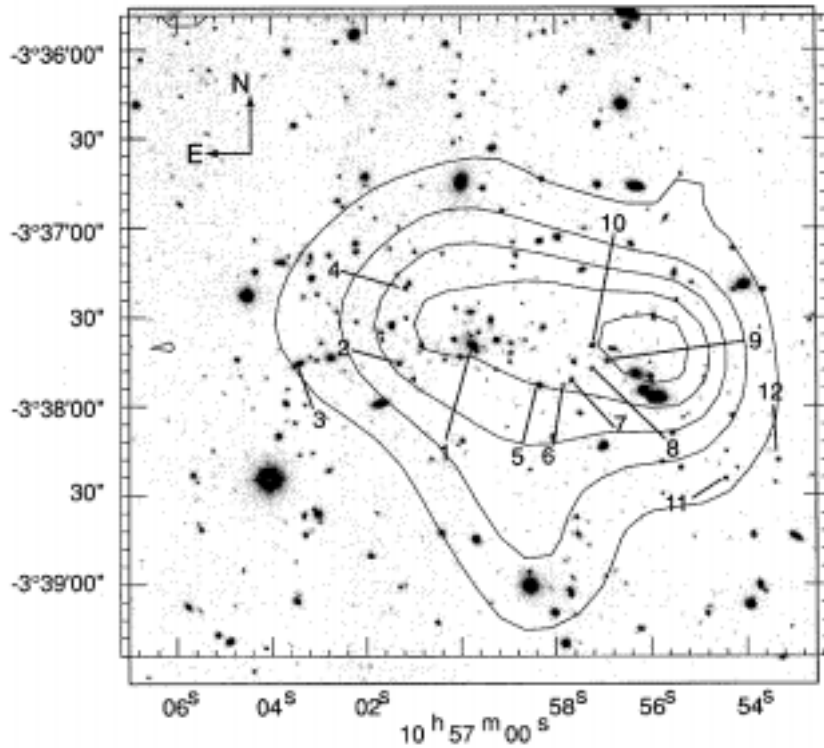


Figure 1. ROSAT X-ray contour map of MS 1054-0321 superposed on I-band image reproduced from [10].

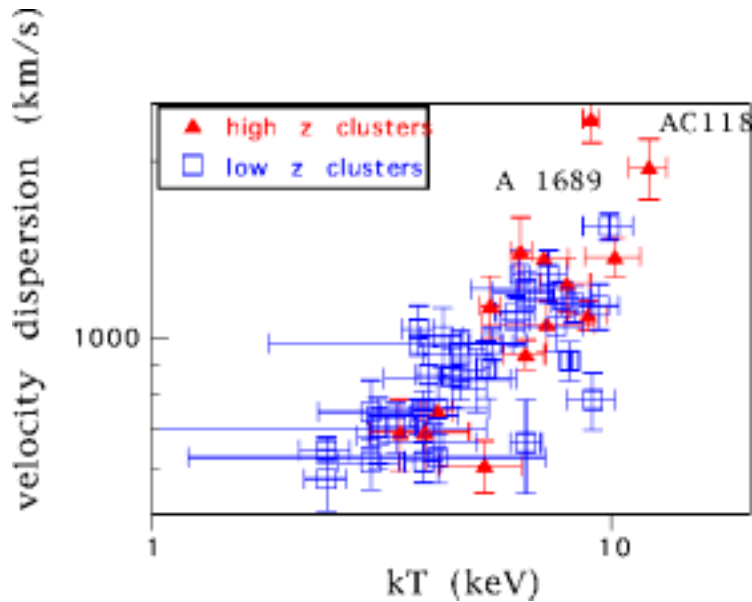


Figure 2. Optical velocity dispersion vs. emission weighted average X-ray temperature for a large sample of low and high ($z > 0.14$) redshift clusters. Note the scatter and the appearance of a few objects with much higher velocity dispersion than expected from the X-ray temperature. The 2 named clusters are objects with strong gravitational arcs. Reproduced from [13]

of the cluster mass [18,19]. Accounting for cooling flows in the analyses also results in the flattening of the relationship between L_{Bol} and T_X to $L_{\text{Bol}} \propto T_X^{2.6 \pm 0.3}$ [20,21]. This relationship is used for examining the evolution of clusters. Models of evolution which assume that gas and dark matter evolve together predict $L_{\text{Bol}} \propto T_X^2$ [22]. Deviation from this relationship implies that the evolution of gas and dark matter is different perhaps due to pre-heating of the gas by mergers of galaxies or supernovae [22]. No evolution is found in the $L_{\text{Bol}} - T_X$ relation within $z \sim 0.4$ [20].

Cooling flow (CF) clusters have been found to have metallicities that are about 1.8 times more compared to metallicities in non-cooling flow (NCF) clusters [23]. This has been suggested to be due to peaked gas density in the center and presence of metallicity gradient in CF clusters. Accretion of gas in the centres of CFs, established from an earlier epoch, leading to a massive star formation in them could be responsible for this. On the other hand NCFs with flatter density distribution show signs of recent merger activity which could have disrupted the cooling flows in them and dispersed the metals more uniformly.

3. Mass estimates

Gravitational masses of clusters have been estimated based on (a) β model eq. (3) from X-ray imaging data and using average temperatures [7]. (b) density and temperature profiles

derived from deprojection analysis of X-ray images eq. (4) [17]. In both cases, the derived mass depends on the outermost limit imaged in X-rays which depends on the sensitivity of the instrument used. In the study by Lewis *et al* [7], total mass determined for a radius of 0.4–0.5 Mpc is in the range $1.8\text{--}3.2 \times 10^{14} h^{-1} M_{\odot}$, and increases almost linearly to $7\text{--}9 \times 10^{14} h^{-1} M_{\odot}$ with distance out to a radius of about 1.3 Mpc, accessible in a limited number of cases. Peres *et al* [17] find masses in the range of $0.25\text{--}2.4 \times 10^{14} h^{-1} M_{\odot}$ for clusters with measurements extending to a radius of 0.5 Mpc. The gas mass fractions range from $5.5\text{--}11.5 h^{-1.5}\%$ (or 11–23% for $h = 1/2$) for $r = 0.5$ Mpc. Lewis *et al* [7] find no systematic bias between these X-ray derived masses and dynamical masses obtained from galaxy velocities, with average $M_{\text{Dyn}}/M = 1.04 \pm 0.07$.

Gravitational lensing provides another method to measure cluster masses that is free from assumptions about the dynamical state of the gravitating matter. Early comparisons between the measurements from this method and those based on X-ray data led to a discrepancy of a factor ~ 2 between the two estimates [24]. The possible reasons given for this discrepancy include: (i) clusters having prolate ellipsoidal mass distributions; (ii) superpositions of mass clumps along the lines of sight which enhance the probability of detecting gravitational arcs and can increase the lensing mass [25]; (iii) non-isothermal temperature structure in X-ray gas; (iv) bulk and/or turbulent motions or magnetic fields providing partial pressure support against intra-cluster medium (ICM); (v) multiphase nature of central ICM (CF regions) resulting in significant differences between emission-weighted and mass-weighted temperatures of clusters and thus biasing mass measurements based on X-rays to lower values. The last part has been explored in great detail by Allen [19] who finds that after the effects of CFs are taken into account, comparisons of two mass estimates in

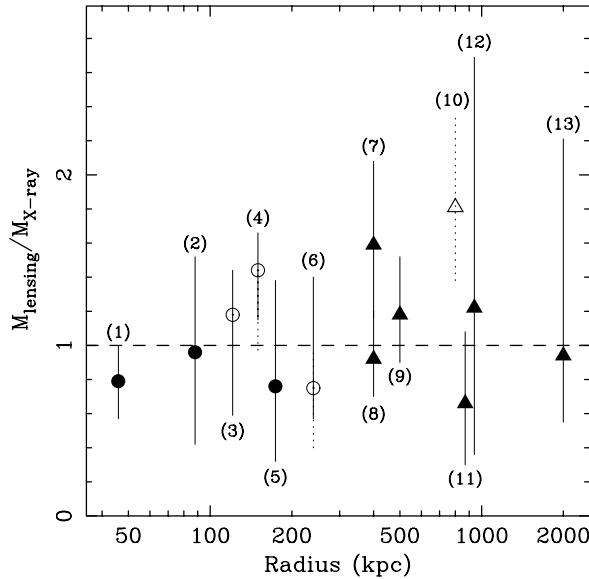


Figure 3. Circles (filled: detailed lens models; open: simple symmetric models) are for clusters with strong lensing and CFs. Triangles (open: A2218) are for weak-lensing results. Reproduced from [19].

clusters with weak gravitational lensing show excellent agreement on large spatial scales (figure 3). Strongly lensing clusters with NCFs, however, still lead to mass estimates that are larger by factor ≥ 2 than the X-ray values (figure 1 of [19]). Similar results have been reported by Lewis *et al* [7].

4. Implications for cosmological parameters

Assuming that clusters are formed due to gravitational collapse from regions of the Universe with representative ratios of baryonic to dark matter, we can infer that the baryon fraction in clusters is equal to that in the field. Baryon fraction, f_b , defined as the ratio of the visible mass in galaxies and intracluster gas to the total cluster mass, therefore, should not differ substantially from the universal value, Ω_b/Ω , when determined near the outer boundary of the cluster [26]. The cosmological density parameter can thus be obtained as $\Omega = \Omega_b/f_b$. Values of Ω_b are constrained by big bang nucleosynthesis models to lie in the range $0.005 < \Omega_b h^2 < 0.015$ [27]. Assuming that X-ray gas is the major component of visible baryons in the clusters, and taking the average value of $f_b = 0.047$ from [7], we get $\Omega = 0.11 - 0.32 h^{-0.5}$. Since baryon fraction, measured only to a limited distance, is known to increase with radius and does have non-negligible contribution from visible galaxies, the range of values for Ω would be further lowered. In any case, $\Omega = 1$, requiring a drop in the gas mass, is not allowed by the data.

White *et al* [28] showed that σ_8 , the rms mass fluctuation amplitude on $8 h^{-1}$ Mpc scale, and Ω are related as $\sigma_8 \Omega^{0.56} \simeq 0.57$ in the cold dark matter (CDM) models with $\lambda = 1 - \Omega$ where λ is the dimensionless cosmological constant. This constraint is not able to distinguish models with $\Omega = 1$ and $\sigma_8 \simeq 0.57$ from models with $\Omega \simeq 0.20$ and $\sigma_8 \simeq 1.25-1.58$. Evolution of cluster abundance as a function of redshift breaks this degeneracy [29]. A general lack of evidence for evolution in cluster properties – X-ray luminosity function

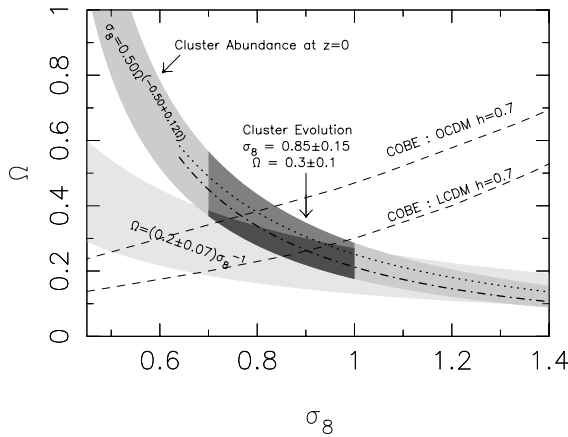


Figure 4. Constraints on cosmological parameters from cluster abundances and COBE results. LCDM refers to N-body simulations for Lambda CDM normalised to COBE results; similarly OCDM refers to Open CDM. Reproduced from [28].

from ROSAT all sky survey for $z < 0.3$ [30] or even upto $z < 0.7$ [8], T_X vs. L_X or T_X vs. σ relationships [31], is consistent with $\Omega < 1$ Universe. In particular, Bahcall *et al* [29] find that mild observed evolution of cluster abundance gives $\sigma_8 = 0.83 \pm 0.15$ and $\Omega \simeq 0.3 \pm 0.1$. The anisotropies in the microwave background detected by COBE also allow the determination of σ_8 which is, however, sensitive to the spectral index of the primordial fluctuation spectrum as well as Ω and λ . The overall constraints on σ_8 and Ω are summarised in figure 4 reproduced from [29].

Existence of a number of very hot (> 8 keV), thus very massive, clusters at redshifts > 0.5 severely challenge models of hierarchical structure formation with $\Omega = 1$. At least 3 such clusters are known: MS0016+16 ($T_X = 8.4$ keV; $z = 0.54$), MS0451-03 ($T_X = 10.4$ keV; $z = 0.54$), and MS1054-0321 ($T_X = 12.3$ keV; $z = 0.83$) [10]. In an $\Omega = 1$ Universe where initial density perturbations are Gaussian, using V/V_{\max} test, the expected number density of such hot clusters at $z = 0.5 - 0.9$ is $\sim 1.6 \times 10^{-8} \text{ h}^3 \text{ Mpc}^{-3}$ [10]. The probability of all 3 clusters appearing in the volume sampled by the EMSS in the $\Omega = 1$ Universe is 10^{-6} [10]. In summary, X-ray studies of clusters strongly favour a low Ω Universe.

Acknowledgements

I wish to thank the organisers for holding a successful workshop on ‘Cosmology : Observations Confront Theories’, their invitation to give this talk, and their hospitality. I thank S W Allen, N A Bahcall, M Donahue and R F Mushotzky for permission to reproduce their figures here.

References

- [1] G O Abell, H G Corwin and R P Olowin, *Astrophys. J. Suppl.* **70**, 1 (1989)
- [2] F Zwicky, E Herzog, P Wild, M Karpowicz and C T Kowal, *Catalogue of galaxies and cluster galaxies*, vols 1–6, (1961–68)
- [3] D A White and A C Fabian, *Mon. Not. R. Astron. Soc.* **273**, 72 (1995)
- [4] H Ebeling, A C Edge, H Bohringer and S W Allen *et al.*, **301**, 881 (1998)
- [5] H Ebeling, W Voges, H Bohringer, A C Edge, J P Huchra and U G Briel, *Mon. Not. R. Astron. Soc.* **283**, 1103 (1996)
- [6] I M Gioia, J P Henry, T Maccacaro, S L Morris, J T Stocke and A Wolter, *Astrophys. J.* **356**, L35 (1990)
- [7] A D Lewis, E Ellingson, S L Morris and R G Carlberg, astro-ph/9901062 (1999)
- [8] C Scharf, L R Jones, H Ebeling, E Perlman, M Malkan and G Wegner, *Astrophys. J.* **477**, 79 (1997)
- [9] L R Jones, C Scharf, H Ebeling and E Perlman *et al.*, *Astrophys. J.* **495**, 100 (1998)
- [10] M Donahue, G Mark Voit, I Gioia, G Luppino, J P Hughes and J T Stocke, *Astrophys. J.* **502**, 550 (1998)
- [11] A Cavaliere and R Fusco-Femiano, *Astron. Astrophys.* **49**, 137 (1976)
- [12] I King, *Astrophys. J.* **174**, L123 (1972)
- [13] R F Mushotzky, Colloquium on *The age of the Universe, dark matter and structure formation* (National Academy of Sciences, USA, 1998)
- [14] N A Bahcall and L M Lubin, *Astrophys. J.* **426**, 513 (1994)
- [15] M Markevitch, W R Forman, C L Sarazin and A Vikhlinin, *Astrophys. J.* **503**, 77 (1998)
- [16] M Lowenstein and R F Mushotzky, *Astrophys. J.* **466**, 695 (1996)

- [17] C B Peres, A C Fabian, A C Edge, S W Allen, R M Johnstone and D A White, *Mon. Not. R. Astron. Soc.* **298**, 416 (1998)
- [18] S W Allen, A C Fabian and J-P Kneib, *Mon. Not. R. Astron. Soc.* **279**, 615 (1996)
- [19] S W Allen, *Mon. Not. R. Astron. Soc.* **296**, 392 (1998)
- [20] S W Allen and A C Fabian, *Mon. Not. R. Astron. Soc.* **297**, L57 (1998)
- [21] M Markevitch, *Astrophys. J.* **504**, 27 (1998)
- [22] N Kaiser, *Astrophys. J.* **383**, 104 (1991)
- [23] S W Allen and A C Fabian, *Mon. Not. R. Astron. Soc.* **297**, L63 (1998)
- [24] J Miralda-Escude and A Babul, *Astrophys. J.* **449**, 18 (1995)
- [25] M Bartelmann and M Steinmetz, *Mon. Not. R. Astron. Soc.* **283**, 431 (1996)
- [26] S D M White, J F Navarro, A E Everard and C S Frenk, *Nature* **366**, 429 (1993)
- [27] K A Olive, Summary of lectures given at the 1997 Lake Louise Winter Institute, Lake Louise, Alberta, astro-ph/9707212 (1997)
- [28] S D M White, G Efstathiou and C S Frenk, *Mon. Not. R. Astron. Soc.* **262**, 1023 (1993)
- [29] N A Bahcall, X Fan and R Cen, *Astrophys. J.* **485**, L53 (1997)
- [30] H Ebeling, A C Edge, A Fabian, S Allen, C Crawford and H Boehringer, *Astrophys. J.* L101 (1997)
- [31] R F Mushotzky and C A Scharf, *Astrophys. J.* **482**, L13 (1997)